

PRECISE GEOREFERENCING IN THE ABSENCE OF GROUND CONTROL: A STRIP ADJUSTMENT APPROACH

C. S. Fraser, M. Ravanbakhsh, M. Awrangjeb

Cooperative Research Center for Spatial Information, Department of Geomatics
University of Melbourne VIC 3010, Australia
[c.fraser, m.ravanbakhsh, mawr]@unimelb.edu.au

KEY WORDS: Sensor modelling, satellite imagery, strip adjustment, RPCs, accuracy evaluation

ABSTRACT:

The options available for orientation of satellite imagery in cases requiring optimal metric precision are generally rational functions, where the RPCs are provided by the image supplier, or a rigorous physical model. In either case, it is ground control that facilitates pixel-level georeferencing via a compensation for systematic errors in the sensor metadata. In many remote parts of the world, where satellites are the most viable source of imagery for mapping, there is a lack of ground control, which thus precludes bias-free georeferencing. This paper reports on a practical means of overcoming this problem, namely the orientation of long strips of imagery through a bundle adjustment process that requires ground control at the endpoints only. The adjustment utilises a rigorous sensor orientation model. RPCs are then generated for each scene within the strip of images from the adjusted sensor orientation data. These facilitate bias-free georeferencing without reference to ground control. The approach discussed has previously proven successful for automated orthoimage generation from ALOS imagery, and in this paper its application to a 7-scene strip of QuickBird imagery is reported.

1. INTRODUCTION

High-resolution satellite imagery (HRSI) has proven to be a valuable data source for medium and large scale topographic mapping. Georeferencing and associated functions such as orthoimage generation and feature extraction can be performed to pixel level and even sub-pixel accuracy. Options for sensor orientation in cases requiring optimal metric precision are generally either rational functions, where the rational polynomial coefficients (RPCs) are provided with the imagery, or a rigorous physical model. In either case, it is the provision of good quality ground control points (GCPs) that facilitates the pixel-level georeferencing via a compensation for systematic errors in the sensor metadata. These errors are usually associated with orbit and attitude biases. In many remote parts of the world, where the use of HRSI is the only viable means to provide imagery for mapping, there is a lack of ground control, which thus precludes bias-free georeferencing.

A practical means of overcoming this problem can be found in an approach involving the precise orientation of long strips of imagery through an orientation adjustment process that requires ground control at only the endpoints. The adjustment utilises a rigorous sensor orientation model, but the parameters of this model are not necessarily conducive to exploitation by standard photogrammetric workstations. Thus, in order to further photogrammetrically process imagery forming the strip, RPCs are generated for each scene from the adjusted sensor orientation. These facilitate bias-free georeferencing without reference to ground control – other than the modest number of GCPs employed for the strip adjustment. Pixel-level mapping accuracy is thus facilitated.

The long-strip adjustment approach, first reported in Rottensteiner et al. (2008; 2009), was recently adopted for automated orthoimage generation from ALOS PRISM and AVNIR-2 imagery by GeoScience Australia, leading to increases in production of close to 300% (Fraser et al., 2008). In

this paper, application of the strip adjustment approach to Quickbird imagery is evaluated.

Figure 1 provides an overview of the workflow for the overall strip adjustment scenario for QuickBird. The process starts with input of the imagery, all from the same orbital pass, and its metadata. Strip orientation is then carried out once the image measurement of 3D ground points is completed. Finally, RPC coefficients are generated using the adjusted, bias-free orientation parameters for each of the images forming the strip.

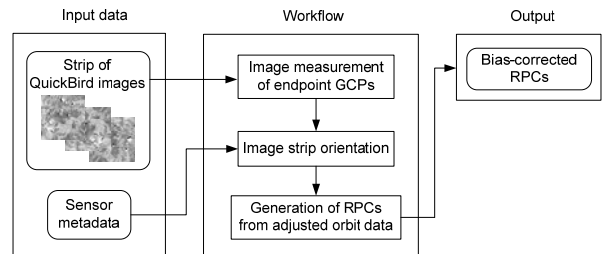


Figure 1. Workflow for strip adjustment approach.

In the following sections, the sensor orientation model employed for the strip adjustment (Weser et al, 2008a;b) is first described, along with the necessary process to adapt QuickBird metadata to this generic model. This is followed by a brief description of the process by which successive scenes are merged into a single strip with one set of orbit and attitude correction parameters. The process of RPC generation is also briefly touched upon. An experimental application of the long-strip image orientation for QuickBird imagery is then discussed.

2. SENSOR ORIENTATION

2.1 Generic orientation model

The sensor orientation model used for the strip adjustment is now overviewed to provide a basis for the discussion of how

Quickbird metadata is accommodated within the generic model. Further details are provided in Weser et al. (2008a;b).

The physical model for a pushbroom satellite imaging sensor relates a point $\mathbf{P}_{ECS} = (X_{ECS}, Y_{ECS}, Z_{ECS})^T$ in an earth-centered object coordinate system to the position of its projection $\mathbf{p}_I = (x_I, y_I, 0)^T$ in an image coordinate system. The scanner records each image row consecutively at time t , so the coordinate y_I of an observed image point directly corresponds with the recording time t through $t = t_0 + \Delta t \cdot y_I$, where t_0 is the time of the first recorded image row and Δt the time interval for recording a single image row. The framelet coordinate system, in which the observation \mathbf{p}_I can be expressed as $\mathbf{p}_F = (x_F, y_F, z_F)^T = (x_F, 0, 0)^T$, refers to an individual CCD array. The relationship between an observed image point \mathbf{p}_F and the object point \mathbf{P}_{ECS} is given as

$$\mathbf{p}_F = \mathbf{c}_F + \mu \cdot \mathbf{R}_M^T \cdot \{\mathbf{R}_P^T(t) \cdot \mathbf{R}_O^T \cdot [\mathbf{P}_{ECS} - \mathbf{S}(t)] - \mathbf{C}_M\} - \delta \mathbf{x} \quad (1)$$

Here, $\mathbf{c}_F = (x_F^C, y_F^C, f)$ describes the position of the projection centre in the framelet coordinate system. Its coordinates are usually referred to as the parameters of interior orientation: the principal point (x_F^C, y_F^C) and the focal length f . The vector $\delta \mathbf{x}$ formally describes corrections for systematic errors such as velocity aberration and atmospheric refraction. It can also be expanded to model camera distortion or other systematic error effects. The shift \mathbf{C}_M and the rotation matrix \mathbf{R}_M describe a rigid motion of the camera with respect to the satellite. They are referred to as the camera mounting parameters.

The satellite orbit path is modelled by time-dependant functions, ie $S(t) = [X(t), Y(t), Z(t)]^T$, and the sensor attitudes are described by a concatenation of a time-constant rotation matrix \mathbf{R}_O and a matrix $\mathbf{R}_P(t)$. These are parameterised by time-dependant functions describing three rotation angles, *roll*(t), *pitch*(t) and *yaw*(t). The components of the orbit path and the time-dependant rotation angles are in turn modelled by cubic spline functions. The rotation matrix \mathbf{R}_O rotates from the earth-centred coordinate system to one that is nearly parallel to the satellite orbit path and can be computed from the satellite position and velocity at the scene centre.

2.2 Model for QuickBird

The transformation parameters relating the object coordinates \mathbf{P}_{ECS} of a point to its *detector coordinates* \mathbf{p}_D (Digital Globe, 2006) are provided in the Quickbird metadata. The detector coordinates are defined in a way that is similar to the framelet system used in the generic model, except for a 90° rotation around the Z_F -axis, so $\mathbf{p}_D = \mathbf{R}_{Z90}^T \cdot \mathbf{p}_F$ (Weser et al., 2008a). The relationship between \mathbf{P}_{ECS} and \mathbf{p}_F can then be given as

$$\mathbf{P}_{ECS} = \mathbf{S}(t) + \mathbf{R}_Q^T(t) \cdot [\mathbf{C}_{MQ} + \lambda \cdot \mathbf{R}_{MQ}^T \cdot (\mathbf{R}_C^T \cdot \mathbf{R}_{Z90}^T \cdot \mathbf{p}_F + \mathbf{p}_F^\theta + \delta \mathbf{x}_Q)] \quad (2)$$

There are several differences between Eqs. 1 and 2. In Eq. 2 there is no orbit coordinate system and thus no rotation matrix \mathbf{R}_O . The defined rotation matrices are transposed compared to those appearing in Eq. 1, and $\mathbf{R}_Q(t)$ and \mathbf{R}_{MQ} are parameterised by quaternions. The framelet coordinate system is rotated by both \mathbf{R}_{Z90}^T and a rotation \mathbf{R}_C^T around the Z_F -axis. The coordinates \mathbf{p}_F^θ of the origin of the framelet coordinate system in the QuickBird camera system are then given, instead of the framelet coordinates \mathbf{c}_F of the projection centre. With the corrections $\delta \mathbf{x}_Q$ applied in the camera coordinate system, Eq.2 becomes

$$\begin{aligned} \mathbf{P}_{ECS} = \mathbf{S}(t) + \mathbf{R}_Q^T(t) \cdot [\mathbf{C}_{MQ} + \lambda \cdot \mathbf{R}_{MQ}^T \cdot \mathbf{R}_C^T \cdot \mathbf{R}_{Z90}^T \cdot (\mathbf{p}_F + \mathbf{R}_{Z90} \cdot \mathbf{R}_C \cdot \mathbf{p}_F^\theta + \mathbf{R}_{Z90} \cdot \mathbf{R}_C \cdot \delta \mathbf{x}_Q)] \end{aligned} \quad (3)$$

Formulae for determining \mathbf{c}_F and $\delta \mathbf{x}$ from the parameters given in the QuickBird metadata can be derived from Eqs. 1 and 3:

$$\mathbf{c}_F = -\mathbf{R}_{Z90} \cdot \mathbf{R}_C \cdot \mathbf{p}_F^\theta \quad (4)$$

$$\delta \mathbf{x} = \mathbf{R}_{Z90} \cdot \mathbf{R}_C \cdot \delta \mathbf{x}_Q \quad (5)$$

The rotation matrix $\mathbf{R}_Q^T(t)$ in Eq. 2 rotates from the object coordinate system to one whose Z -axis points to the target, i.e. the system is not tangential. The rotation matrix $\mathbf{R}_{MQ}^T \cdot \mathbf{R}_C^T \cdot \mathbf{R}_{Z90}^T$ rotates into the camera system. $\mathbf{R}_Q^T(t)$ has to be split into two rotations. In order to achieve a platform coordinate system that is close to a tangential system, $\mathbf{R}_P(t)$ is defined to be equal to the identity matrix for the acquisition time t_c of the image centre, thus $\mathbf{R}_P(t_c) = \mathbf{I}$. The matrix \mathbf{R}_O in Eq.1 is computed from the orbit positions and velocities at time t_c . A comparison of Eqs. 1 and 3 yields $\mathbf{R}_Q^T(t_c) \cdot \mathbf{R}_{MQ}^T \cdot \mathbf{R}_C^T \cdot \mathbf{R}_{Z90}^T = \mathbf{R}_O \cdot \mathbf{R}_P(t_c) \cdot \mathbf{R}_M = \mathbf{R}_O \cdot \mathbf{R}_M$ for $t = t_c$. Thus, the camera mounting rotation matrix \mathbf{R}_M can be computed from the parameters given in the QuickBird metadata as

$$\mathbf{R}_M = \mathbf{R}_O^T \cdot \mathbf{R}_Q^T(t_c) \cdot \mathbf{R}_{MQ}^T \cdot \mathbf{R}_C^T \cdot \mathbf{R}_{Z90}^T \quad (6)$$

Using the shorthand $\mathbf{p}_C = \mathbf{p}_F + \mathbf{R}_{Z90} \cdot \mathbf{R}_C \cdot \mathbf{p}_F^\theta + \mathbf{R}_{Z90} \cdot \mathbf{R}_C \cdot \delta \mathbf{x}_Q$, Eq.3 can be re-written as

$$\begin{aligned} \mathbf{P}_{ECS} = \mathbf{S}(t) + \mathbf{R}_O^T(t) \cdot \mathbf{R}_Q(t_c) \cdot \mathbf{R}_O \cdot [\mathbf{R}_O^T \cdot \mathbf{R}_Q^T(t_c) \cdot \mathbf{C}_{MQ} + \\ + \lambda \cdot \mathbf{R}_O^T \cdot \mathbf{R}_Q^T(t_c) \cdot \mathbf{R}_{MQ}^T \cdot \mathbf{R}_C^T \cdot \mathbf{R}_{Z90}^T \cdot \mathbf{p}_C] \end{aligned} \quad (7)$$

$$= \mathbf{S}(t) + \mathbf{R}_Q^T(t) \cdot \mathbf{R}_Q(t_c) \cdot \mathbf{R}_O \cdot [\mathbf{R}_O^T \cdot \mathbf{R}_Q^T(t_c) \cdot \mathbf{C}_{MQ} + \lambda \cdot \mathbf{R}_M \cdot \mathbf{p}_C]$$

The remaining parameters in Eq. 1 are then given by

$$\mathbf{C}_M = \mathbf{R}_O^T \cdot \mathbf{R}_Q^T(t_c) \cdot \mathbf{C}_{MQ} \quad (8)$$

$$\mathbf{R}_P(t) = \mathbf{R}_O^T \cdot \mathbf{R}_Q^T(t) \cdot \mathbf{R}_Q(t_c) \cdot \mathbf{R}_O \quad (9)$$

Eq. 9 has to be applied to each of the discrete data points provided for the satellite attitudes, and the angles $roll^{obs}(t)$, $pitch^{obs}(t)$, $yaw^{obs}(t)$ derived from $\mathbf{R}_P(t)$ are used in the adjustment.

2.3 Bundle adjustment

The aim of bundle adjustment is to improve the parameters of the sensor model formulated in Eqs. 1 and 2 using the framelet coordinates of image points, the corresponding object coordinates of GCPs, and direct observations for the orbit path and attitudes derived from the metadata. The coefficients of the spline functions that model the time-dependant components of the orbit path $\mathbf{S}(t)$ and the time-dependant rotational angles parameterising $\mathbf{R}_P(t)$ are also determined. The adjustment model is expanded by bias-correction parameters which model the systematic errors in direct observations for the orbit path and attitude angles. For each orbit parameter p (the coordinate of an orbit point or a rotation angle), a time-constant unknown Δp is introduced. The observation p^{obs} recorded at time t^{obs} is related to the spline $S_p(t)$ describing the parameter p by

$$S_p(t^{obs}) = p + \Delta p \quad (10)$$

Six systematic error correction parameters per satellite orbit result, and these have to be determined along with the spline parameters, which comprise three offsets $(\Delta X, \Delta Y, \Delta Z)^T$ for the

orbit path points and three offsets $(\Delta roll, \Delta pitch, \Delta yaw)^T$ for the rotation angles.

2.4 Strip adjustment

In the case of either single-orbit stereo imagery or three-line scanner imagery, such as with ALOS PRISM, the bundle adjustment can directly yield 3D ground point coordinates from corresponding observed image point pairs or triplets. However, the long-strip adjustment approach is also applicable to continuous strips of non-stereo imagery, as illustrated by Fig. 2. Indeed, the refinement of the sensor orientation for such long strips is seen as its principal application. For these configurations, the term *bundle adjustment* is perhaps a little misleading, since what is essentially being performed is more akin to a *spatial resection* from GCPs in that there is no direct computation of the ground coordinates of any measured image point.

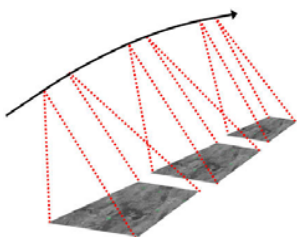


Figure 2. Apparent scene merging for long-strip image orientation.

The first step in the strip adjustment process involves an initial merging of scenes along with their associated orbit and attitude data. A single set of camera mounting and interior orientation parameters then applies for the orientation of what may now be thought of as a single composite image (even though no actual image merging occurs or is necessary). Also, the six bias correction parameters for orbit path and attitude relate to the entire ‘multi-scene image’. The resulting adjusted orientation and bias-correction parameters for the strip can then be mapped back to the individual scenes to refine their orientation.

3. RPC GENERATION

As already mentioned, it needs to be recognized that the measurement of tie points between adjacent images is not necessary in the strip adjustment approach, unlike the situation with traditional aerial triangulation of frame imagery. The long-strip adjustment should be viewed as a means of adjusting sensor orbit and attitude. This corrected orientation data is then delivered to the user in the form of newly generated RPCs. Actual 3D georeferencing (eg via monoplotting) can then follow as a separate, as opposed to integral part, of the strip adjustment process.

The RPC model, as computed using camera and sensor orientation parameters, is universally accepted as an alternative sensor orientation model for HRSI (eg Fraser et al., 2006). RPCs facilitate the transformation from image to object space coordinates in a geographic reference system. However, for reasons primarily due to issues of numerical conditioning within the process of generating the 80-odd polynomial coefficients, the actual expressions comprising the quotients of two third-order polynomials usually relate normalised (scaled and offset) line and sample coordinates to normalised latitude, longitude and ellipsoidal height.

Within the long-strip adjustment scenario, RPCs are generated for each of the images forming the strip, such that bias-free georeferencing and associated processes (eg orthoimage generation) can subsequently take place on standard photogrammetric workstations. While such commercial systems might be able to directly ingest orbit and attitude data from the Quickbird metadata files, it is very unlikely they will be able to accommodate the sensor orientation corrections generated within the long-strip adjustment. The generation of bias-corrected RPCs offers a means to circumvent this problem.

4. EXPERIMENTAL TESTING

A strip of seven 60cm-resolution Quickbird Basic images covering an area in northeast New Zealand was employed both to further validate the orientation formulation for Quickbird, Eq. 3, and experimentally test the long-strip adjustment process. Each image covered an area of approximately $16.5 \text{ km} \times 16.5 \text{ km}$, with the resulting strip being approximately 95km in length (scenes overlapped to a small extent). All scenes were near nadir, the average off-nadir angle being 10° . The imagery was recorded in August, 2008.

In the area covered by the seven scenes, 21 3D ground points were available. The geographic coordinates of these survey marks, which were to serve as GCPs and checkpoints, had been surveyed with a nominal sub-meter horizontal and vertical accuracy. However, in spite of there being site photographs of the survey marks, which were available via the website of Land Information New Zealand, none of the points were of sufficient definition in the images to be measurable to better than an estimated accuracy of a few pixels. This presented an unfortunate impediment to any fully comprehensive analysis of the accuracy potential of the Quickbird strip adjustment, and the authors could only verify metric performance of the adjustment process, again to the ‘few pixel’ level. For this reason, the results of the testing will be presented here as a broad summary. Further analysis awaits the provision of either better GCP/Checkpoint data or an alternative Quickbird image strip.

Image coordinates were measured using the *Barista* software system for HRSI data processing (Barista, 2009) and image merging, strip adjustment, RPC regeneration and subsequent georeferencing were also performed using *Barista*.

A set of four GCPs were selected for the adjustment, two at each end of the 95km long strip, as shown in Fig. 3. This figure also indicates the locations of the remaining 17 points that served as checkpoints for accuracy assessment in a subsequent georeferencing via newly generated RPCs. Note that most of the checkpoints were situated in the central part of the strip, where the largest positional errors would be expected.

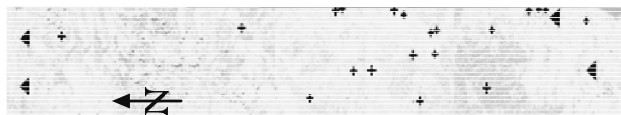


Figure 3. Distribution of 3D points along the 95km strip; GCPs are shown by triangles and checkpoints by crosses.

As a first step in the strip adjustment process, the orbit data for all scenes was merged, such that only one set of spline parameters and one set of error correction parameters for sensor orbit and attitude were employed for the entire strip. Following the adjustment, the 17 checkpoints were back-projected into the

images using the estimated orientation parameters. Their positions were then compared to the measured image point locations. There were 24 comparisons made, due to some checkpoints falling in the overlap area between adjacent scenes. Consistent results were found, with randomly distributed discrepancies at the 1-4 pixel level (recall that these are indicative only given the poor checkpoint information). In spite of the less than desirable quality of the ground point data, the results were sufficient to provide a measure of confidence that the strip adjustment approach was producing improved, bias-free orientation data for each image.

Positional discrepancies in planimetry could also be quantified in object space via monoplotting with the adjusted image orientation data, with the result being, again, an RMS error of ‘a few metres’. As a final accuracy check, monoplotting was again carried out via the generated RPCs. Here, there was a high degree of consistency in the results from the two monoplotting operations, the discrepancies in Easting & Northing coordinates being less than 0.2m for all points. This verified the integrity of the RPC generation process, but it unfortunately did not shed any more light on the absolute accuracy of the georeferencing.

5. CONCLUDING REMARKS

In spite of the fact that it was not possible with the experimental data provided to carry out a comprehensive accuracy evaluation of the strip adjustment procedure for Quickbird imagery, all indications were that this practical approach to achieving bias-free image orientation over long strips of imagery with minimal ground control was performing to expectations. Previous application to ALOS PRISM and AVNIR-2 imagery had demonstrated the advantages of the long-strip image orientation method (Rottensteiner et al., 2009; Fraser et al., 2008) and the results reported here, in spite of the shortcomings in definitively quantifying accuracy aspects, suggest that the strip adjustment approach is equally applicable to QuickBird imagery.

ACKNOWLEDGEMENTS

The authors express their gratitude to Sinclair Knight Merz Pty Ltd, Spatial Division for making the strip of Quickbird imagery available.

REFERENCES

- Barista, 2009. Barista product information webpage, <http://www.baristasoftware.com.au> [Accessed: 3 March 2008].
- Digital Globe, 2006. *QuickBird Imagery Products – Product Guide*. http://www.digitalglobe.com/downloads/QuickBird_Imagery_Products - Product_Guide.pdf [Accessed: 17 Feb. 2009].
- Fraser, C. S., Weser, T., Rottensteiner, F., 2008. Image merging to support georeferencing and orthoimage generation from ALOS imagery. *29th Asian Conference on Remote Sensing*, ACRS, Colombo, 8 pages (on CDROM).
- Fraser, C. S., Dial, G., Grodecki, J., 2006. Sensor orientation via RPCs. *ISPRS Journal of Photogrammetry and Remote Sensing*, 60(3): 182-194.
- Rottensteiner, F., Weser, T. and Fraser, C.S., 2008. Georeferencing and orthoimage generation from long strips of ALOS imagery. *Proceedings of 2nd ALOS PI Symposium*, ESA/JAXA, Rhodes, Greece, 3-7 Nov., 8 pages (on CDROM).
- Rottensteiner, F., Weser, T., Lewis, A. & Fraser, C.S., 2009. A Strip Adjustment Approach for Precise Georeferencing of ALOS Imagery. *IEEE Transactions on Geoscience and Remote Sensing* (in press)
- Weser, T., Rottensteiner, F., Willneff, J., Poon, J. & Fraser, C. S., 2008a. Development and testing of a generic sensor model for high-resolution satellite imagery. *Photogrammetric Record*, 21(123): 255-274.
- Weser, T., Rottensteiner, F., Willneff, J. & Fraser, C. S., 2008b. An improved pushbroom scanner model for precise georeferencing of ALOS PRISM imagery. *Intern. Arch. Photogrammetry, Remote Sensing & Spatial Information Sci.*, Beijing, XXXVII (B1-2): 723-730.